DIFFERENTIAL JET PRODUCTION CROSS SECTION MEASUREMENT IN Z + JET EVENTS FROM PROTON - PROTON COLLISIONS AT $\sqrt{S}$ = 13 TEV USING THE CMS DETECTOR AT LHC

by

Ashley Marie Parker

August 2019

A dissertation submitted to the
faculty of the Graduate School of
the University at Buffalo, The State University of New York
in partial fulfilment of the requirements for the degree of

Doctor of Philosophy

Department of Physics

Table of Contents

List of Tables

List of Figures

Abstract

In The standard model of particle physics, while describing our universe well on many scales, has yet to be precisely measured in all energy regimes. Recent theoretical advances in higher order QCD calculations have provided a way to compare the standard model's predictions to precision measurements of data and monte carlo simulation. Within this dissertation, I present a measurement of the double differential jet production cross section as a function of the jet mass and transverse momentum, in events with a Z + Jet topology, with and without a jet grooming algorithm applied. Studying Z + jet events will yeild a light quark enriched jet sample, which has not yet been studied at $\sqrt{s}$ = 13 TeV.

Furthermore, comparing groomed and ungroomed jets will allow us the better understand the jet mass in all energy regimes since the groomed jets will have varying amounts of soft and collinear radiation with respect to the ungroomed counterpart.For ungroomed jets, leading-order and next-to-leading order QCD Monte Carlo programs are found to predect the jet mass spectrum in the data reasonably well, with some disagreement at very low and very high masses. For groomed jets, the agreement between the Monte Carlo programs and the data improves overall, and extends lower in jet mass due to the removal of soft and colinear portions of the jet.First-principles theoretical calculations of the groomed jet mass are also compared to the data, and agree with the data

within the range of acceptability of the calculations.

Ultimately these measurements will be used to tune Monte Carlo generators, producing more accurate parton showering simulations, leading to tighter constraint of backgrounds in future searchs for new physics.

Chapter 1

Theoretical Framework

1.1 Introduction To The Standard Model

"Theorists can be wrong; only nature is always right" - David Gross

The Standard Model, SM, of particle physics constitues humanity's most rigorous theory of our universe, providing predictions of observables which have since been measured, in the case of Quantum Electrodynamics, QED, to the highest precision of any scientific theory. Despite the impressive predictions,the gravitational force and more subtle phenomena, such as flavor oscillation of neutrinos [5], indicate the existence of physics Beyond the Standard Model, BSM.

The known particles of the SM are; 6 types of quark and 6 types of lepton, which comprise matter, and the guage bosons, which mediate the 3 (this theory does not yet encompass gravitaion) fundamental forces; The strong and weak nuclear interactions and electromagnetism.

Various attempts have been made to unify the fundamental forces under one

theory, thusfar the electromagnetic and weak interactions have been united by electro-weak theory.

The Standard electroweak model can be described $SU(2)xU(1)$ mathematically.

The $SU(2)xU(1)$ guage group is a convolution ($<$ $-$That is not the right word...) of the special unitary symmetry group $SU(2)$ describing 3 mixed massive vector bosons, W_- W_+ Z_0, carriers of the weak nuclear force and the unitary gauge group $U(1)$, describing the lonely massless chargeless photon, of the electromagnetic interaction.

The standard model of the strong interaction is known as quatum chromodynamics, QCD, a non-Abelian guage theory described by the special unitary group $(SU(3)_f)$, where the flavours of quark are the physical manifestation of the symmetry group. This force is mediated by the 8 massless gluons which carry color charge, making QCD more complicated mathematically than QED.

The SM also contains a Higgs boson, an excitation of a scalar Higg's field, which gives rise to spantaneous symmetry breaking of the electroweak theory, providing the particles with mass, but I won't get into that.

The quarks and leptons are arranged in generations according to their relative masses, as shown in Figure 1.2. The table also shows the spins of the particles, the leptons and quarks have half-integer spin, fermions, that obey the fermi exclusion principle, conversely the bosons have half integer spin and therefore obey bose-einstein statitics. Through the SM we interpret the observed hadronic particles, mesons (baryons) , as 2 quark (3 quark) bound states. The existence of spin $\frac{3}{2}$ baryons, which are symmetric bound states in space, spin and flavour and the need to obey Fermi-Dirac statistics, by maintaining total assymmetry of the wavefunction,implies there is another degree of freedom, called color, so

that each quark is either red, green or blue. Granted only color singlet, containing either all 3 or 1 and it's anti color, states exist. Furthermore there exists a property of asymptotic freedom where the QCD coupling between quarks and gluons increases as they asymptotically approach one another. There exists a wealth of experiemental data to support the concept of asymptotic freedom despite the fact that rigorous mathematical proof of the exlusion of free quark and gluon states has yet to be acheived.

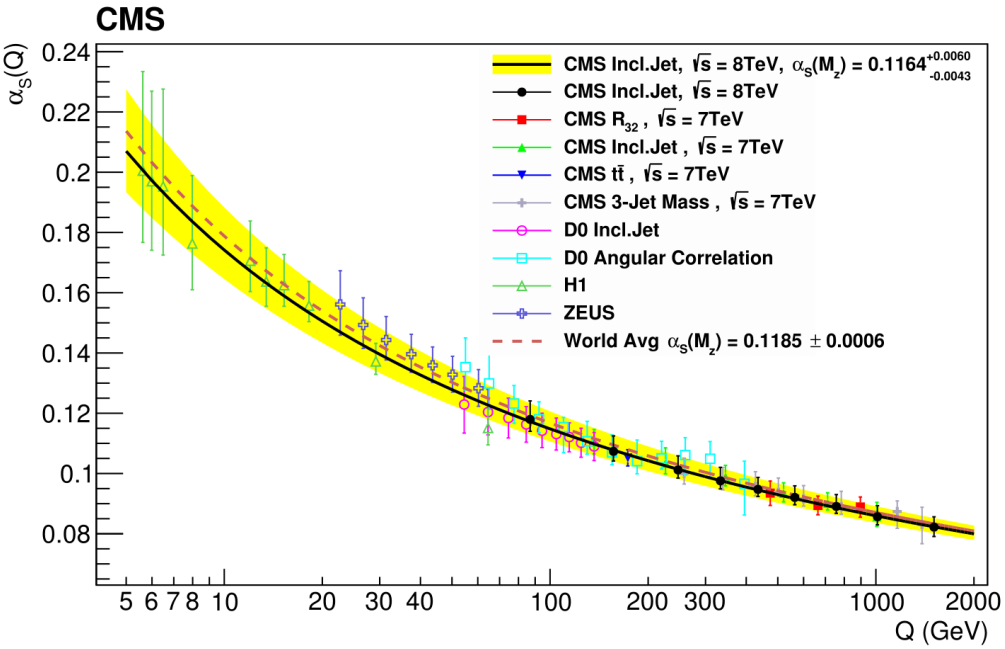

Figure 1.1: The running of the strong coupling constand as compiled by CMS including measurements from CMS and HERA among others [1].

Assymptotic freedom is a useful property as it allows for perturbative calculations of QCD observables, this is discussed in section XXX.

Nuclei in ordinary matter are composed solely of 1^{st} generation particles, up and down quarks, bound by gluons. Neutral atoms contain an equal number of protons (composed of 2 up quarks and a down quark) and electrons, 1^{st} generation leptons. The main distinction between leptons and quarks, both fermions

(particles of $\frac{1}{2}$ integer spin), being that leptons do not experience the color interaction $(SU(3)_f)$ like their quark friends. In each generation there is a quark with charge $Q = +\frac{2}{3}$ (up, charm, top) and another of charge $Q = -\frac{1}{3}$ (down, strange, bottom).

1.1.1 Quantum Chromodynamics

lagrangian

$$\mathcal{L} = -\frac{1}{4} F^A_{\mu\nu} F^{\mu\nu}_A + \sum_{\text{flavours}} \overline{\psi}_a \left(i\gamma_\mu D^\mu - m \right)_{ab} \psi_b \tag{1.1}$$

$$F^A_{\mu\nu} = \partial_\mu A^A_\nu - \partial_\nu A^A_\mu + g_s f^{ABC} A^B_\mu A^C_\nu \tag{1.2}$$

covariant derivative

$$\left(D_\mu\right)_{ab} = \partial_\mu \delta_{ab} - i g_s A^A_\mu t^A_{ab} \tag{1.3}$$

In order to emphasize the relevance to the measurement presented herein, the theory of Quantum Chromodynamics is discussed here from a kinematic (¡-better word?) rather than Lagrangian perspective. This is useful as jet studies help probe QCD in the soft and collinear limits. Jets are formed by the hadronization of quarks and gluons. In this thesis I present a measurement of a light quark enriched jet sample.

Consider the simplest process that could produce a quark initiated jet, a quark of energy E_q emitting a gluon of energy E_g. The probability that this will occur is a function of the gluon's energy fraction, z, and the emission angle , θ [6].

$z = \frac{E_g}{E_q + E_g}$

$1 - cos\theta = \frac{m^2}{2E_q E_g}$

Then the probability of gluon emission from the quark is :
$P_q(z, cos\theta) dz dcos\theta = \frac{\alpha_s C_F}{\pi} \frac{dz}{z} \frac{dcos\theta}{1-cos\theta}$

It is useful to assume the small angle approximation, $\theta << 1$, giving:

$P_q(z, \theta^2) dz d\theta^2 = \frac{\alpha_s C_F}{\pi} \frac{dz}{z} \frac{d\theta^2}{\theta^2}$

Notice that the probability of emission diverges for very soft (small z) or very collinear (small θ) gluons. In the soft and collinear limits the probability can be interpretted as an expectation value for the number of soft/collinear gluons [6].

It is elucidating to rewite the probability in terms of inverse logarithms in the and intruduce the "Lund Diagram" in order to visualize the uniform distribution of soft and collinear gluons in the $log\frac{1}{\theta^2}, log\frac{1}{z}$ space.

The primary lund plane is shown in Figure XX [3]
$P_q(z, \theta^2) dz d\theta^2 = \frac{\alpha_s C_F}{\pi} d(log\frac{1}{z}) d(log\frac{1}{\theta^2})$

Jets can also be initiated by gluons and this probability is incredibly similar :
$P_q(z, \theta^2) dz d\theta^2 = \frac{\alpha_s C_A}{\pi} d(log\frac{1}{z}) d(log\frac{1}{\theta^2})$

This similarity allows us to interpret the variations in quark enriched and gluon enriched jet samples in terms of the fundamental C_F and adjoint C_A

casimirs, in $SU(3)$, $C_F = \frac{4}{3}$ and $C_A = 3$.

Comparing the probability of a quark to emit a gluon and that of a gluon to to emit a gluon, we can see the ratio is simply $\frac{C_A}{C_F} = \frac{9}{4}$. This has strong experimental implications since it implies gluon jets will on average be composed of about twice as many constituent particles as quark jets.

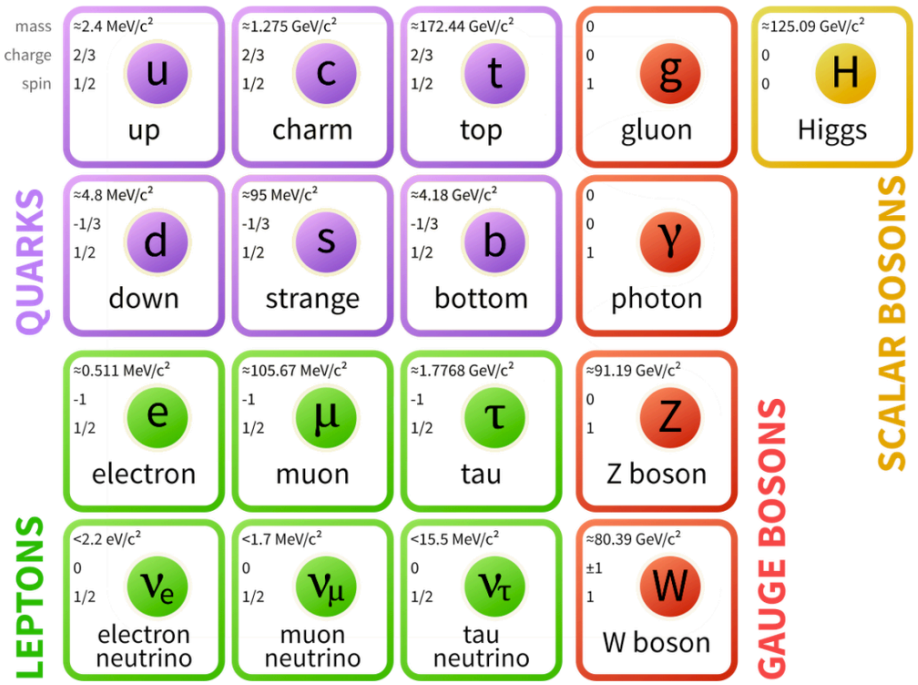

Figure 1.2: Fundamental particles of the Standard Model [2].

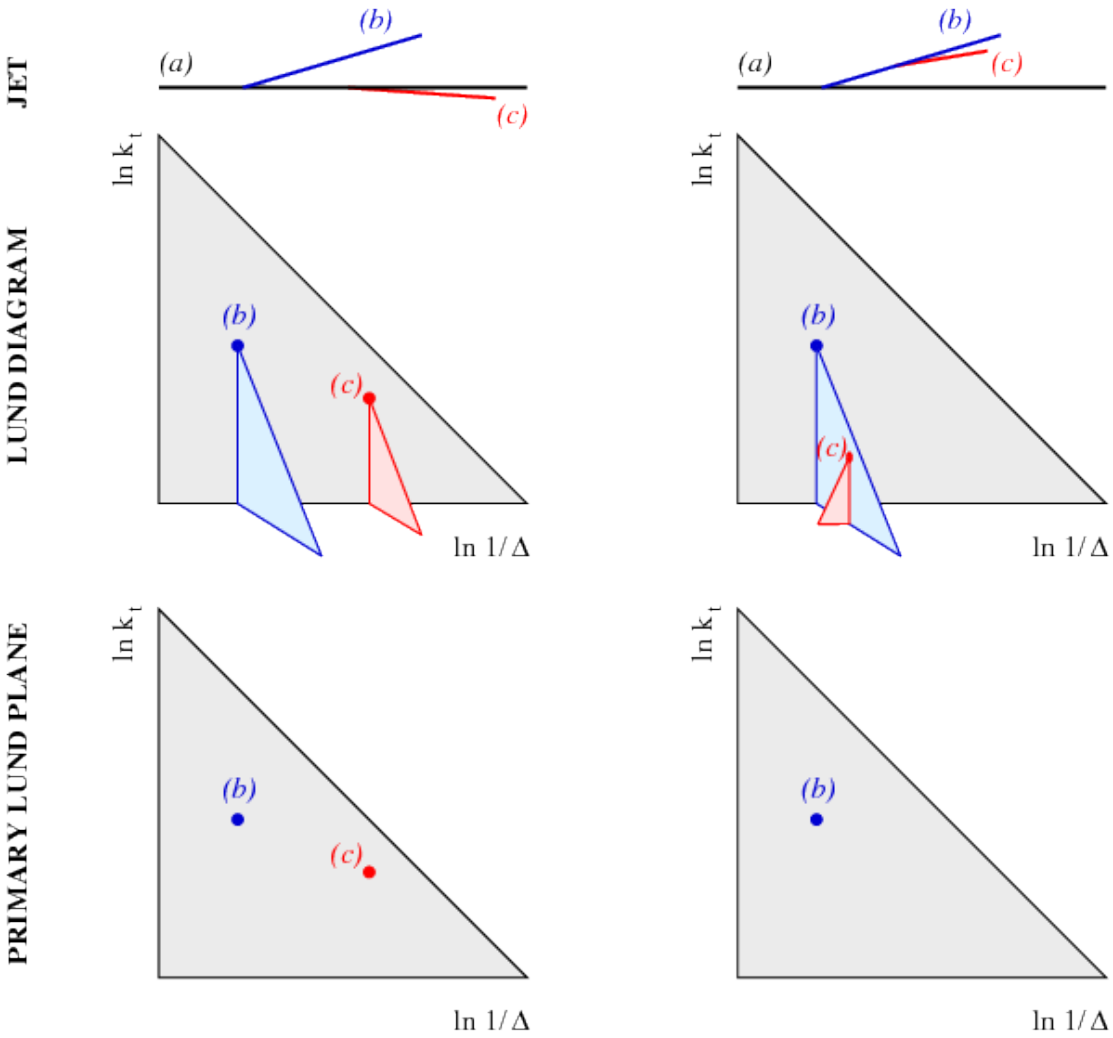

Figure 1.3: The primary and secondary lund planes for 2 example jets [3].

Chapter 2

Jets in Proton-Proton Collisions

A jet is a collimated grouping of hadrons usually associated with the production of a parton, quark or gluon, in this case initiated by the hard scatter of 2 constituent partons from protons. The initial parton radiates other quarks and gluons, called the "Parton Shower" and all color charged particles fragment into hardons, mainly pions and kaons, before reaching the detector.

Studies of jets at LHC are complicated by experimental complexities such as "underlying event", other partons from the same proton iteracting and depoiting energy in the same region of the detector. "Pileup" is also increasingly relevant, like "underlying event" but initiated from other proton interactions from this or a previous bunch since LHC collides 10^{11} protons in bunches every 25 nanoseconds.

Lastly any measurement is limited by the resolution of the measurement device and any detector effects which are disentangled from the signal by "unfolding" the reconstructed distributions back to generator level.

While jets are often used as simple proxies for the quark or gluon from which they originated, the structure of the radiation pattern of the hard scatter is en-

coded within the jet's constituent particles [7]. Jet studies are essential for a complete understanding of proton-proton interactions since the majority of interesting physics signatures contain a color charged parton in the final state. This chapter covers the basics of jet physics at LHC, from the algorithms used for clustering the constituent particles in experimental data to the language and calculations of the theory.

2.1 Jet Clustering Algorithms

Ideally, a jet represents a quark [gluon] parton however a more precise definition :

"A phase space region (as defined by an unambiguous hadronic fiducial cross section measurement) that yields an enriched sample of quarks [gluons] (as interpreted by some suitable, though fundamentally ambiguous, criterion)" [8] as defined at the Les Houches confernece in 2015 .

I will discuss one class of "suitable, though fundamentally ambiguous" criteria for defining jets, known as sequential recombination algorithms. These algorithms take pairs of particles and successively combine them into 1 particle, in a way which in intended to reconstruct the successive branchings of partons within the jet as described by perturbative QCD [9].

In sequential recombination algorithms a distance metric, d_{ij}, is defined between all particle pairs, these pairs are then sequentially combined in order of increasing distance.There exist three popular algorithms in this class, all of the following can be described by the equation [10]:

$$
\begin{aligned}
d_{ij} &= \min\left(p_{ti}^{2p}, p_{tj}^{2p}\right)\frac{\Delta R_{ij}^2}{R^2} \quad \Delta R_{ij}^2 = \left(y_i - y_j\right)^2 + \left(\phi_i - \phi_j\right)^2 \\
d_{iB} &= p_{ti}^{2p}
\end{aligned}
\tag{2.1}
$$

Depending on the value chosen for p, this equation can produce a variety of clusterings, herein I discuss the 3 popular choices $p = [1, 0, -1]$ refering to them by their names ; KT [10], Cambridge/Aachen [11] and Anti-KT algorithms [12], respectively.

KT - ¿ C/A -¿ Anti-KT [13]

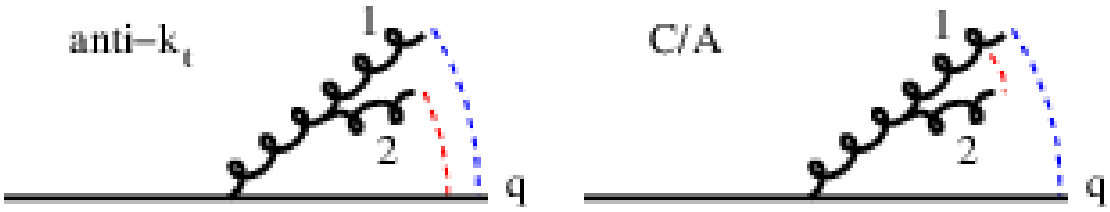

Figure 2.1: How clustering follows radiation pattern for different algorithms [3].

2.2 Jet Structure

The picture is not so simple, we have pileup and underlying event. We analyze the entire radiation pattern and from its structure can determine the probability that a gluon or quark (even the type of quark) initiated this jet there exist many methods for going about these tasks.

Quark/Gluon discrimination is discussed in section QUARK GLUON SECTION and can be done in many ways such as examining the gluon emission spectrum as visualized in the lund plane as mentioned in the introduction. In this section quark jet discrimination is discussed, specifically how the higher order corrections to the hard process are nessessary in order to properly predict measurements in the non-perturbative regime.

NLO + NLL + NP to match data in non-perturbative regime

[14]

[7]

2.3 Jet Grooming

Soft-drop

other grooomers

image of soft drop compared to others

image of soft drop grooming tree

2.4 Jet Production Cross Sections

$$\sigma = \sum_{a,b} \int_0^1 dx_a dx_b \int d\Phi_n f_a^{h_1}(x_a, \mu_F) f_b^{h_2}(x_b, \mu_F) \frac{1}{2\hat{s}} \left|\mathcal{M}_{ab\to n}\right|^2 (\Phi_n; \mu_F, \mu_R) \quad (2.2)$$

2.5 Jet and Soft Functions in Soft-Collinear Effective Theory

Below the factorization structure of the double differential jet production cross section is displayed in the context of Soft-Collinear Effective Theory, SCET, following the framework for inclusive jet production $pp \to jet + X$ developed in for jets of

$$\frac{d\sigma}{dp_T dm} = \sum_{abc} f_a(x_a, \mu) \otimes f_b(x_b, \mu) \otimes H_{ab}^c(x_a, x_b, p_T/z, \mu) \otimes \mathcal{G}_c(z, p_T R, m, \mu, z_{\text{cut}}, \beta) \quad (2.3)$$

Image of factorization in this context

[4] discuss groomed jets in this context

comparing groomed (Jet) to ungroomed (Jet+Soft)

2.6 Jets Initited by Quarks and Gluons

earlier discussed $C_F = \frac{4}{3}$ and $C_A = 3$

CITE A Theory of Quark vs. Gluon Discrimination

Dijets make quark gluon admixture Z+Jets make mostly light quark jets, studied here and in 7 TeV analysis (1 D unfolding there and no soft drop)

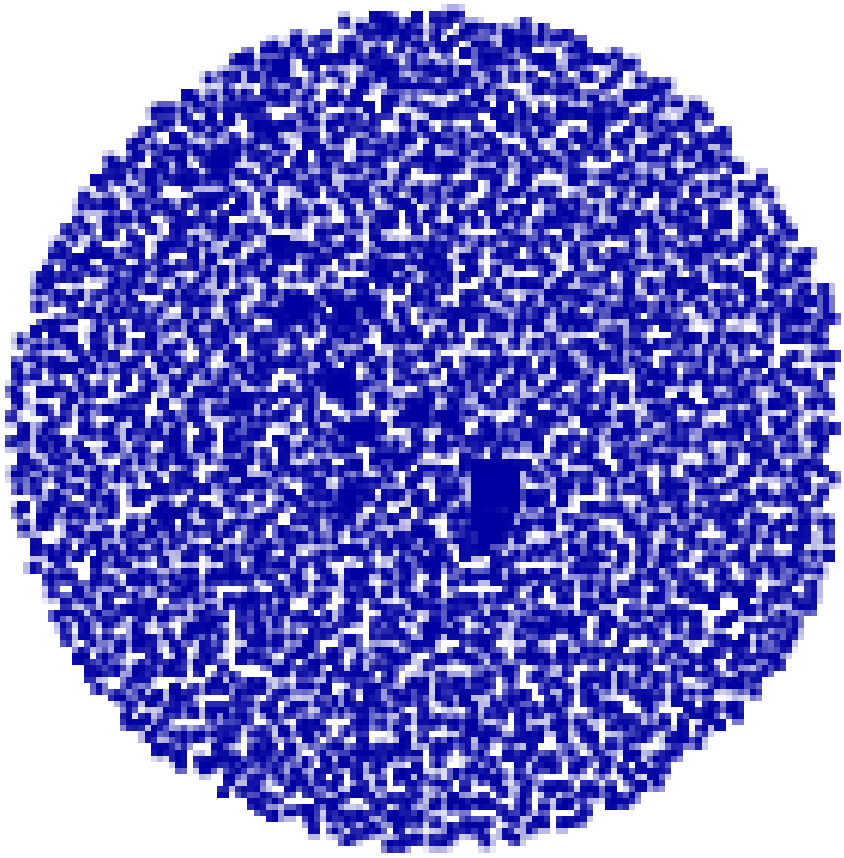

Figure 2.2: How clustering looks for Anti-Kt, circular pattern makes pileup and underlying event subtraction more simple for experimentalists [3].

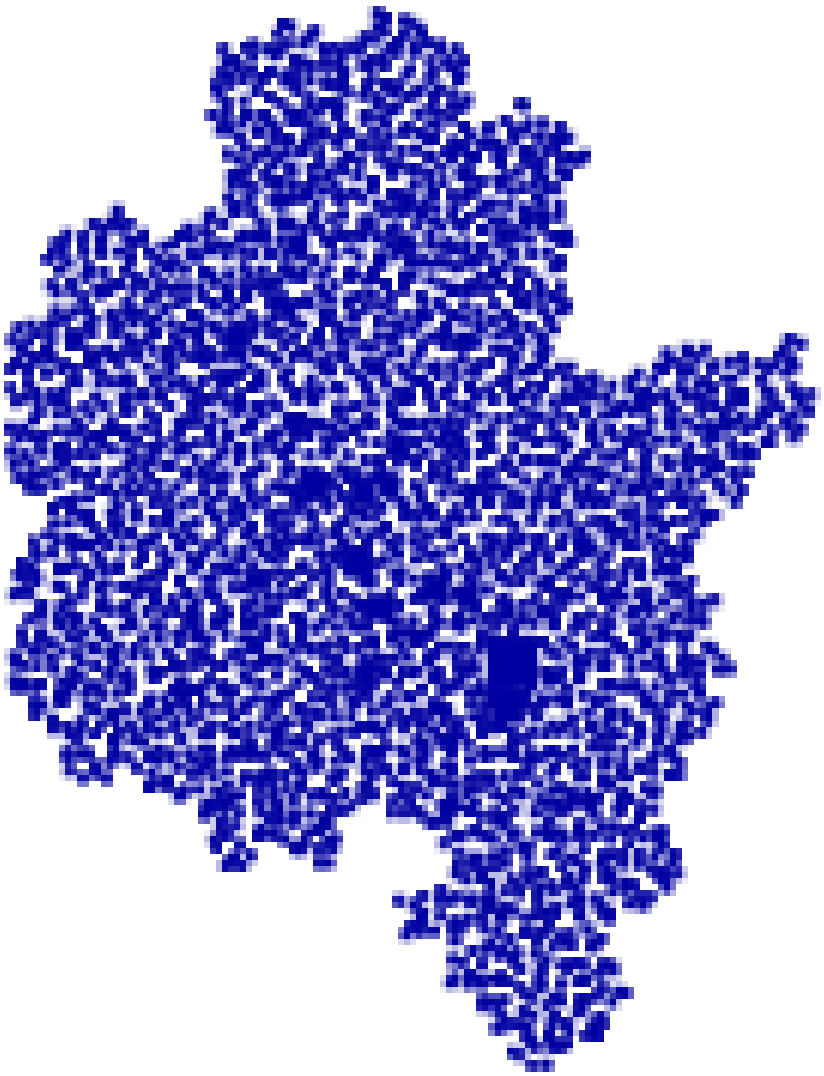

Figure 2.3: C/A, not circular, shaped like radiation pattern [3].

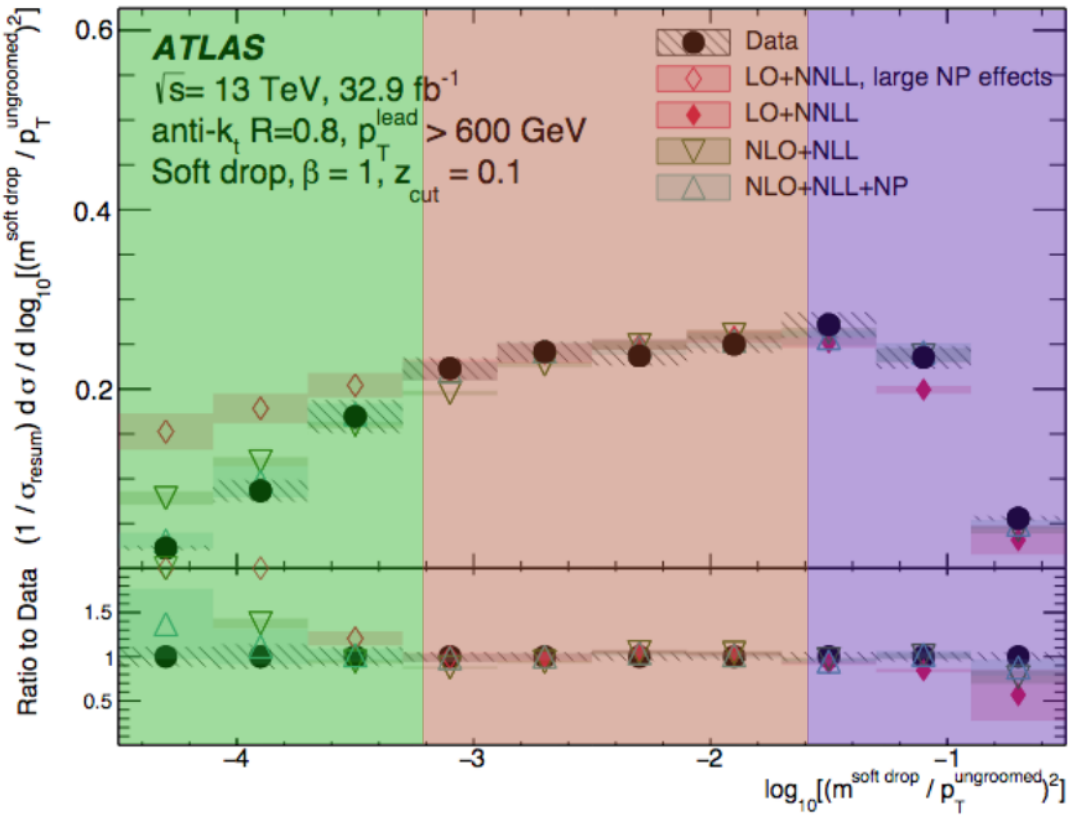

Figure 2.4: ATLS DIJets Rho result [3].

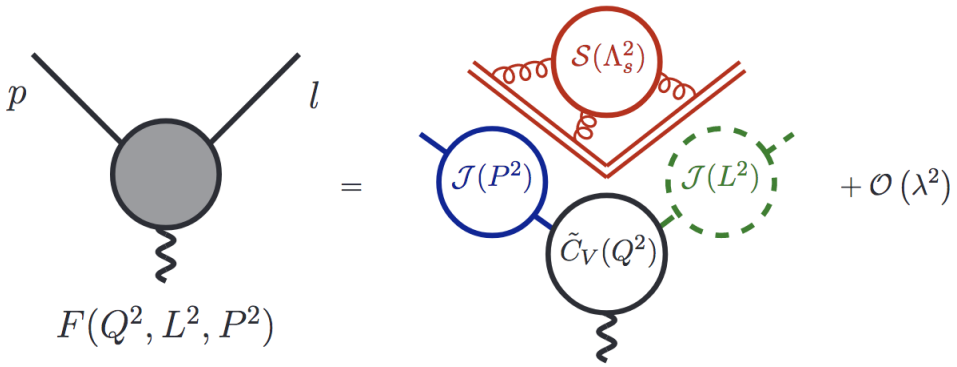

Figure 2.5: Fatorization of the energy scales in a hard scatter interaction according to SCET [4].

Chapter 3

CMS Experiment at LHC

3.1 The Large Hadron Collider

The Large Hadron Collider, LHC, is the largest machine created my mankind.

3.2 The Compact Muon Solenoid

The Compact Muon Solenoid, CMS, is one of 4 detectors that measure collisions of protons and lead ions produced by the Large Hadron Collider, LHC, at CERN. CMS is the smaller of the 2 large general-purpose detectors, the other being ATLAS. The most notable feature of the detector is it's powerful 3.8 Tesla solenoid magnet, the largest superconducting magnet ever built, as of the year 2011.

Chapter 4

Measurement of the differential jet production cross section with respect to jet mass and transverse momentum in Z + Jet events from pp collisions at $\sqrt{s}$ = 13 TeV

Chapter 5

Identification and Calibration of Boosted Hadronic W Bosons within Fully Merged Top Quark Jets at 13 TeV

Chapter 6

Conclusion

6.1 Conclusion

The measurement matches the theoretical calculations well, i hope.

The End.

Bibliography

[1] Vardan Khachatryan et al. Measurement of the inclusive 3-jet production differential cross section in protonproton collisions at 7 TeV and determination of the strong coupling constant in the TeV range. *Eur. Phys. J.*, C75(5):186, 2015.

[2] modellinginvisible.org standard model description. `https://www.modellinginvisible.org/standard-model/`. Accessed: 2019-08-06.

[3] Frdric A. Dreyer, Gavin P. Salam, and Grgory Soyez. The Lund Jet Plane. *JHEP*, 12:064, 2018.

[4] Thomas Becher, Alessandro Broggio, and Andrea Ferroglia. Introduction to Soft-Collinear Effective Theory. *Lect. Notes Phys.*, 896:pp.1–206, 2015.

[5] Y. Ashie et al. A Measurement of atmospheric neutrino oscillation parameters by SUPER-KAMIOKANDE I. *Phys. Rev.*, D71:112005, 2005.

[6] Andrew J. Larkoski. An Unorthodox Introduction to QCD. 2017.

[7] Lily Asquith et al. Jet Substructure at the Large Hadron Collider : Experimental Review. 2018.

[8] J. R. Andersen et al. Les Houches 2015: Physics at TeV Colliders Standard Model Working Group Report. In *9th Les Houches Workshop on Physics at TeV Colliders (PhysTeV 2015) Les Houches, France, June 1-19, 2015*, 2016.

[9] Simone Marzani, Gregory Soyez, and Michael Spannowsky. Looking inside jets: an introduction to jet substructure and boosted-object phenomenology. 2019. [Lect. Notes Phys.958,pp.(2019)].

[10] Stephen D. Ellis and Davison E. Soper. Successive combination jet algorithm for hadron collisions. *Phys. Rev.*, D48:3160–3166, 1993.

[11] Yuri L. Dokshitzer, G. D. Leder, S. Moretti, and B. R. Webber. Better jet clustering algorithms. *JHEP*, 08:001, 1997.

[12] Matteo Cacciari, Gavin P. Salam, and Gregory Soyez. The anti-k_t jet clustering algorithm. *JHEP*, 04:063, 2008.

[13] Jeff Tseng and Hannah Evans. Sequential recombination algorithm for jet clustering and background subtraction. *Phys. Rev.*, D88:014044, 2013.

[14] Gavin P. Salam. Towards Jetography. *Eur. Phys. J.*, C67:637–686, 2010.